ELSEVIER

Journal of Alloys and Compounds 256 (1997) 76–81

Journal of ALLOYS AND COMPOUNDS

Magnetoresistance studies of $La_{0.6}M_{0.07}Ca_{0.33}MnO_3$ (M=Er, Yb, Bi) perovskites

D. Bahadur[a], M. Foldeaki[b], S.K. Mandal[a], M.H. Yewondwossen[c], Z. Koziol[c], R.A. Dunlap[c,*]

[a]Department of Metallurgical Engineering and Materials Science, Indian Institute of Technology, Powai, Bombay 400 076, India
[b]Institut de Recherche sur l'Hydrogène, Université du Québec à Trois-Rivières, Trois-Rivières, Québec, Canada G9A 5H7
[c]Department of Physics, Dalhousie University, Halifax Nova Scotia, Canada B3H 3J5

Received 24 October 1996

Abstract

Magnetotransport and magnetic properties of the system $La_{0.6}M_{0.07}Ca_{0.33}MnO_3$ (M=Er, Yb, Bi) have been investigated. The behavior of the three samples varies much more than might be expected on the basis of the similarity in ionic radii of M^{3+} ions and a small quantity of the substitution. A strong correlation is found between magnetization data, FMR and transport behavior. These results are discussed in terms of minor variations in lattice properties and differences in chemical properties, such as ionic radii and electronegativity, which influence the exchange mechanisms. The Bi containing compound is particularly interesting from an applications stand point, as it shows a sharp transition at around 265 K. © 1997 Elsevier Science S.A.

Keywords: Manganese perovskite oxides; Magnetoresistance; Electrical transport; FMR

1. Introduction

Recently, there has been extensive activity to investigate and understand the large magnetoresistance effect in polycrystalline manganese based perovskite oxides [1–4]. It is known that $LaMnO_3$ is an antiferromagnetic insulator and that it transforms to a metallic ferromagnet as a function of substitution at lanthanum sites by divalent alkali ions, such as Ca^{2+} or Sr^{2+}. Doped charge carriers (e.g., holes) mediate the ferromagnetic interaction between localized spins through the double exchange mechanism [5–8]. The ferromagnetic Curie temperature is related to the strength of the exchange integral between $Mn^{3+/4+}$ ions and this influences the electronic conductivity. In the ABO_3 perovskites, crystallographic distortion is introduced by substitution of different sized ions at the A sites. The degree of distortion is expressed in terms of the tolerance factor, t, defined as $t=(R_A+R_O)/\sqrt{2}(R_B+R_O))$, where R_A, R_B and R_O are ionic radii of A, B and oxygen ions respectively. Such distortion may result in the simultaneous presence of canted ferromagnetic and antiferromagnetic spin structures and is believed to be the principal mechanism responsible for the giant magnetoresistance (GMR) effect in such perovskite oxides [9–12]. It follows that in such a system a clear relationship between magnetic, electronic and structural properties should be expected. A typical example of such a manifestation is $La_{0.6}Y_{0.07}Ca_{0.33}MnO_3$ which exhibits a GMR effect which is at least three orders of magnitude larger than that in $La_{0.67}Ca_{0.33}MnO_3$ [13]. The effect of a small amount of yttrium substituted for La is remarkable. Following along this line, we have recently investigated La–Er–Ca–Mn–O based perovskites with small variations in erbium and calcium content to determine the effect of both the lattice properties as well as the change in Mn^{3+}/Mn^{4+} ratio [14]. In a continuation of this work, we report here the magnetoresistance and magnetic properties of the system $La_{0.6}M_{0.07}Ca_{0.33}MnO_3$ with M=Er, Yb and Bi. Ionic radii of Er^{3+}, Yb^{3+} and Bi^{3+} as given by Shannon and Prewitt [15] are 1.00, 0.985 and 1.11 Å, respectively, as compared to 1.32 Å for La^{3+}, and this provides a systematic method for investigating the effects of A site substitutions.

2. Experimental methods

Samples of $La_{0.6}M_{0.07}Ca_{0.33}MnO_3$ with M=Er, Yb and Bi were prepared by mixing the required amount of either oxides or carbonates of the different constituent elements

*Corresponding author.

PII S0925-8388(96)03008-3

and heating very slowly up to 1225 K and holding at that temperature for a period of 6 h. The decomposed powder was again mixed and was pelletized and the pellet was heated to 1725 K for 6 h in air and then cooled slowly to room temperature. These three samples with substitution of Er, Yb and Bi will be referred to in the text as samples E, Y and B, respectively.

The X-ray diffraction patterns were recorded with a Siemens D-500 scanning diffractometer using Cu-Kα radiation. The electrical resistivity and magnetoresistivity were measured as a function of temperature between 4.2 and 300 K and in applied magnetic fields up to 5.0 Tesla. Temperature dependent magnetization measurements were performed between 4.2 and 330 K using a conventional d.c. SQUID (Superconducting Quantum Interference Device) magnetometer in an applied field of 1.0 Tesla.

Ferromagnetic resonance (FMR) studies have been done on rectangular samples with approximate dimensions of 2.0×1.0×0.4 mm at a frequency of 9.1 GHz using a Varian Associates EPR spectrometer over the temperature range 77 to 298 K. The samples were mounted at the center of a rectangular TE waveguide and FMR spectra were recorded for two different geometries; with the applied field parallel and perpendicular to the long axis of the sample.

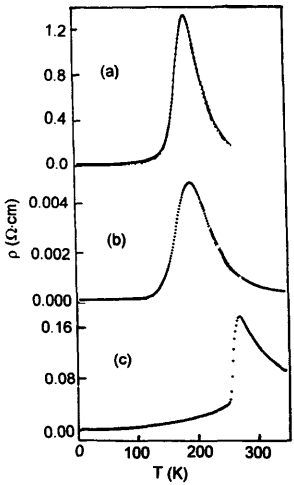

Fig. 1. Zero field resistivity as a function of temperature for samples (a) E, (b) Y and (c) B.

3. Results

X-Ray diffraction results show that all three samples are of the single phase perovskite structure. Table 1 gives the composition, measured lattice parameter, average ionic radius at the A site and the tolerance factor, t, for these three samples. The lattice parameter is the largest for sample Y and goes in the order Y>E>B. On the contrary, the ionic radius of Bi^{3+} is the largest and the ionic radii of the 3+ ions have the order B>E>Y. The size of Bi^{3+} may vary depending upon the degree of $6s^2$ lone pair character. When the Bi^{3+} ion resides in a high symmetry site its size is smaller than La^{3+}, while for a higher degree of lone pair character, its size is larger than La^{3+} [16]. Another possible reason for this discrepancy could be variations in the Yb and Bi valence states. It is known that Yb and Bi can also exist in 2+ and 5+ states, respectively, with ionic radii of 1.14 and 0.85 Å.

Fig. 1 shows the plot of zero field resistivity as a function of temperature for the three samples. All the samples exhibit a maxima above which semiconductor-like behavior is observed, while below this temperature, positive $\partial\rho/\partial T$ is seen. The sample B exhibits the highest transition temperature at around 260 K. Compared to the behavior of the other samples studied here, the transition in sample B is also remarkably sharp. The transition temperatures for samples E and Y and their behavior above the transition temperature are essentially similar. However, the behaviors of the three samples below the transition are somewhat different and this correlates well with their magnetic data, as discussed later in the text. The resistivity as a function of temperature for sample Y in different applied fields up to 5.0 Tesla is illustrated in Fig. 2. This shows a shift in the maxima to higher temperatures as the field increases, indicating a spin dependent mechanism responsible for these effects. This behavior is consistent with that typically seen in related GMR perovskites [14]. Fig. 3 shows a plot of $\Delta\rho/\rho=[\rho(B)-\rho(B=0)]/\rho(B=0)$ as a function of the applied magnetic field for the three samples where $\rho(B)$ and $\rho(B=0)$ are the in-field and zero field resistivities, respectively. The magnetoresistivity ratio (MR) is defined to be $[\rho(B=5\ \mathrm{T})-\rho(B=0)]/\rho(B=0)$ where $\rho(B=5\ \mathrm{T})$ is the resistivity in an applied field of 5.0 Tesla. Values of the MR at 4.2 K are shown in Table 2. The table also gives resistivity values measured at 4.2 K and values of the transition temperature, T_c, as determined by the maximum in the zero field resistivity. While the MR for sample Y is around 85%, sample B shows a MR of only about 35%. It is of relevance to point out that sample B

Table 1
Measured lattice parameters, a, of the elementary perovskite cell, average ionic radii of the A site atoms, $<r_A>$, and calculated tolerance factors, t, of the samples studied in this work

Sample	Composition	a (Å)	$<r_A>$ (Å)	t
E	$La_{0.6}Er_{0.07}Ca_{0.33}MnO_3$	3.8505	1.1356	0.9480
Y	$La_{0.6}Yb_{0.07}Ca_{0.33}MnO_3$	3.8526	1.1342	0.9474
B	$La_{0.6}Bi_{0.07}Ca_{0.33}MnO_3$	3.8415	1.1433	0.9518

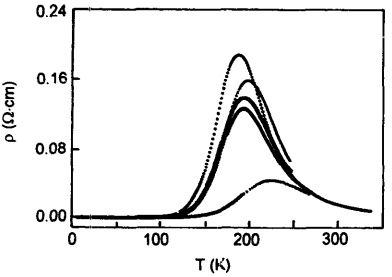

Fig. 2. Resistivity as a function of temperature for different field values for the sample Y. Curves with decreasing peak height correspond to applied fields of 0, 0.5, 1.0, 2.0, and 5.0 Tesla, respectively.

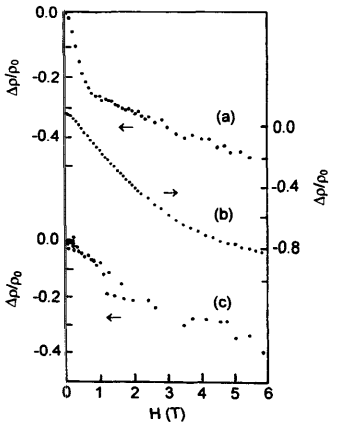

Fig. 3. $\Delta\rho/\rho$ as a function of applied magnetic field at 4.2 K for samples (a) E, (b) Y and (c) B.

exhibits a resistivity (at 4.2 K) at least one order of magnitude smaller than sample E and Y (see Fig. 1 and Table 2). The large scatter in the magnetoresistivity data for the B sample is possibly due to this smaller resistivity value. Plots of magnetization as a function of temperature in a field of 1 Tesla are shown in Fig. 4. Table 2 gives

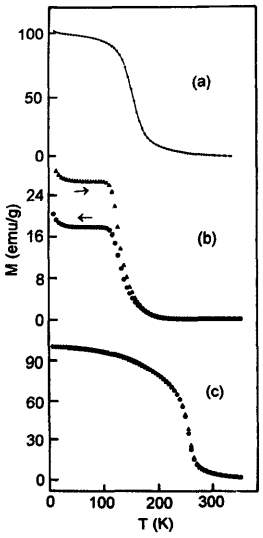

Fig. 4. Temperature dependence of magnetization in a field of 1.0 Tesla for samples (a) E, (b) Y and (c) B.

values of the saturation magnetization at 4.2 K and the transition temperature as obtained from the magnetization curve. These temperatures are in good agreement with the values obtained from the resistivity studies. Samples E and B exhibit typical ferromagnetic behavior with a sharp transition to the paramagnetic state while sample Y exhibits more complex magnetic behavior.

The FMR spectra for the three samples in both parallel and perpendicular configurations at 298 K are shown in Fig. 5. The temperature dependence of the FMR spectra for sample $La_{0.6}Er_{0.07}Ca_{0.33}MnO_3$ is shown in Fig. 6. At room temperature, a single resonance is observed. With decreasing temperature the resonance field, B_r, decreases. The peak-to-peak linewidth, ΔB_{pp}, is more or less constant above T_c, but below T_c there is considerable broadening of the line, presumably due to the presence of the anisotropy field. Also just below T_c, two resonance peaks are clearly seen; one at higher (>0.25 Tesla) and the other at lower

Table 2
Relevant magnetic and transport characteristics of different samples

Sample	MR (4.2 K)	ρ(4.2 K) (Ω cm)	M (4.2 K)	T_c (K) from $\rho(T)$	T_c (K) from $M(T)$
E	0.84	2.4×10^{-2}	102	185	175
Y	0.82	3.5×10^{-3}	20/28	185	175
B	0.35	7.6×10^{-4}	100	260	265

Zero field cooled and field cooled values of the magnetization are shown for sample Y.

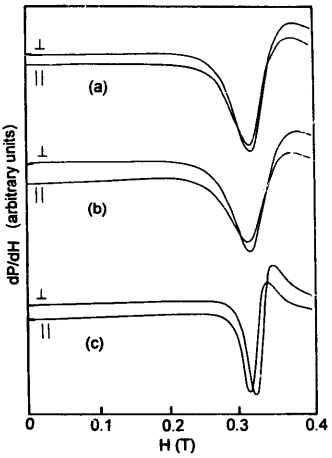

Fig. 5. Ferromagnetic resonance (FMR) spectra recorded in the parallel and perpendicular geometries at 298 K for samples (a) E, (b) Y and (c) B.

(<0.25 Tesla) field. At even lower temperatures the two resonances seem to overlap giving a very broad asymmetric resonance. The low field resonance for sample B is much weaker than the high field resonance. The difference in the resonance field between the parallel and perpendicular field configurations is due to the presence of a demagnetizing field in the samples. Even above T_c, (above the maxima in the resistivity plot) a small shift is observed in the value of B_r when the sample is changed from the parallel to the perpendicular configuration. This may be due to the presence of short range spin ordering above T_c. A similar observation was made by Srivastava et al. [17]. This is also supported by the magnetization curves measured as a function of temperature which show a tail and a small amount of magnetization even above T_c. The room temperature spectra were used to calculate the γ-values for the samples. For parallel and perpendicular resonance, Kittel's equation is modified as [18,19]

$$\left(\frac{\omega}{\gamma}\right)^2 = (H_{\parallel} + H_{an})(H_{\parallel} + H_{an} + 4\pi M) \quad (1)$$

$$\left(\frac{\omega}{\gamma}\right) = (H_{\perp} + H_{an} - 4\pi M), \quad (2)$$

where $B_{\parallel}$ is the resonance field when the magnetic field is applied parallel to the plane of the sample, $B_{\perp}$ is the resonance field when magnetic field is applied perpendicular to the plane of the strip, B_{an} is the anisotropy field, ω is the angular microwave frequency, γ is the gyromagnetic ratio and M is the magnetization at a field of $1/2(B_{\parallel}+B_{\perp})$.

The above equations along with the calculated g-values were used for calculation of the anisotropy field of the samples at different temperatures. The error in the measurements are of the order of ± 1 mT. The values of B_r and ΔB_{pp} both in parallel and perpendicular configurations, as well as B_{an} for the Er, Yb and Bi doped samples are given in Table 3.

A large change in B_r and magnetization values is obvious near the transition temperature. Since the roles of the demagnetizing field and the anisotropy fields in the partially magnetized systems cannot be properly accounted for, there is a considerable amount of uncertainty in the application of Kittel's resonance condition. However, its application has been demonstrated for manganites [20] and other non-saturating systems [18].

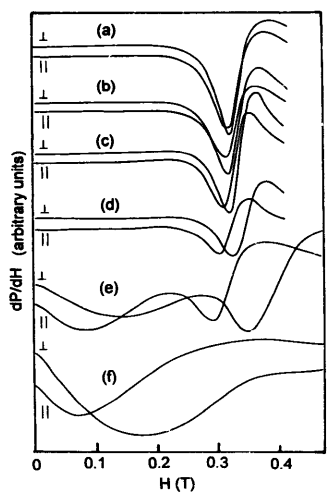

Fig. 6. Ferromagnetic resonance (FMR) spectra recorded in the parallel and perpendicular geometries for sample E at different temperatures; (a) 298 K, (b) 273 K, (c) 223 K, (d) 173 K, (e) 148 K and (f) 123 K.

4. Discussion and conclusions

It is interesting to see a strong correlation between magnetic transitions and the transitions seen in the electrical resistivity data for all three samples. In all three cases the maxima in the resistivity is observed near the temperature where the samples undergo a transition from the magnetically ordered to the paramagnetic state. Such a close resemblance of the electron transport data with the magnetic properties indicates that magnetic spins and their interaction play a crucial role in determining the magneto-

Table 3
Values of ΔB_{pp}, B_r and B_{an} measured using FMR techniques

Sample	g-value	T (K)	ΔB_{pp} (mT)		B_r (mT)		B_{an} (mT)
			∥	⊥	∥	⊥	
E	1.8[a]	298	52	54	344	347	–
		273	50	50	339	343	–
		223	40	40	330	340	14.0
		173	46	52	327	352	15.1
		148	88	150[a]	336	427[a]	–
			138	140	157	210	173.0
		123	282	220	219[b]	290[b]	105.2
Y	1.88	298	64	64	344	348	–
		223	42	42	333	341	13.0
		173	44	50	326	351	14.4
		138	68	–	324	–	–
			102	104	175	232	155.0
		123	244	222	208[b]	311[b]	107.5
B	1.93	298	24	24	328	336	–
		273	38	36	323	358	2.5
		248	100	80	212	360	78.2
			26	64	93	140	228.6
		223	204	210	208[b]	275[b]	107.2

[a] Approximate values.
[b] Two overlapping resonances.

transport behavior. The spin dependent mechanism, which is a function of the Mn^{3+}/Mn^{4+} ratio and their interaction via the oxygen 2p electrons, strongly depends upon the lattice distortion, which in turn is very sensitive to substitutions at the lanthanide site [1,2]. Antiferromagnetic coupling between Mn^{3+} ions in the parent $LaMnO_3$ compound is modified in compounds with A-site substitutions to a layered spin structure with antiferromagnetic coupling between adjacent layers and ferromagnetic order within layers [9]. Therefore, in these systems there is competition between double exchange ferromagnetism and superexchange antiferromagnetism, which may result in a canted antiferromagnetic structure [9,12].

The strength of the ferromagnetic and antiferromagnetic interactions is determined by the overlap of the d orbitals directly or indirectly through the oxygen p orbital, and this is very sensitive to interatomic distances and bond angles [6]. Therefore, very small lattice distortions or changes in the lattice parameter can give rise to combinations of magnetic sublattices determined by different Mn–Mn distances and different Mn–O–Mn bond angles. There have been several reports in the literature where the coexistence of antiferromagnetic and ferromagnetic lattices in these materials has been demonstrated through neutron diffraction and other techniques [9,10]. For instance, Radaelli et al. [10] have shown that the system $La_{0.5}Ca_{0.5}MnO_3$ is a paramagnetic insulator at room temperature which, upon cooling, becomes ferromagnetic at 225 K and antiferromagnetic at 155 K. The plot of magnetization as a function of temperature for sample Y, as shown in Fig. 4, can be attributed to such mixed magnetic behavior. For this sample the transition at around 180 K is clearly due to the ferromagnetic to paramagnetic transition. The abrupt change in the slope of the magnetization curve as well as the change in the irreversible nature of the data at about 115 K is most likely due to a transition from a canted antiferromagnetic structure at lower temperatures to ferromagnetic ordering. The sharp transition seen in both the zero field resistivity and the magnetization data for sample B may be attributed to the existence of only ferromagnetic interactions in this system. In the perovskite lattice, the substitution of a small quantity of atoms with a different ionic radius at the lanthanide site influences the Mn–O–Mn angles much more than the Mn–O–Mn distances in the MnO_6 octahedra, and such subtle changes are known to affect the magnetic and electronic properties remarkably through the modifications of the exchange coupling as suggested earlier [21,22]. When the Mn–O–Mn distances are larger than about 3.8 Å and the distortion of the lattice is minimal, only ferromagnetic order can exist. However, when there is some distortion in the lattice, some of these Mn–O–Mn bond angles may deviate considerably from 180° giving rise to a (canted) antiferromagnetic interaction. This canted antiferromagnetism can, in some cases, be driven to ferromagnetism through the spin flip mechanism by (for example) the application of a magnetic field.

The present FMR results strongly support the above conclusions concerning the magnetotransport and magnetic properties. Near ambient temperature a single resonance with a g-value between 1.86 and 1.93 is observed. The magnetic ions are Mn^{3+} and Mn^{4+} which are in $3d^4$ and $3d^3$ states, respectively. At room temperature there is no magnetic interaction. However, hopping between these ions would still occur. If the hopping frequency is greater than the Larmor frequency, it may lead to a single resonance corresponding to some average field value. At lower temperatures however, due to magnetic interactions, the results are very different. Two well seperated broad resonances are observed. These two resonances below T_c may be attributed to (1) Mn ions participating in ferromagnetic interactions and (2) Mn ions responsible for canted antiferromagnetism which can be driven to ferromagnetic interactions by the application of an applied magnetic field. The low field resonance seems to result from canted antiferromagnetic coupling while the higher field resonance presumably represents the ferromagnetic coupling. The low field resonance is very weak in sample B supporting our observation of mainly ferromagnetic interactions in this sample.

For sample Y, a reduction in magnetization is observed as well as irreversibility below about 115 K between zero field cooled and field cooled magnetization values. Reduced magnetization values and irreversibility are typical characteristics of spin glass behavior. Recently, the system $Pr_{0.7}Ca_{0.3}MnO_3$ has been reported to exhibit similar behavior, and irreversibility was observed below around 80 K between zero field cooled and field cooled magnetization values, this has been attributed to the existence of a spin

glass-like state [9]. These authors have also observed an excellent correlation between the transitions seen in resistivity measurements and changes in the spin structure as observed by neutron diffraction experiments [9].

Sample E exhibits the maximum MR ratio of 84%, whereas sample B exhibits the minimum MR. On the other hand, the transition temperature for sample B is maximum. The following comments can be made concerning this behavior. It is known that spin dependent scattering is the physical origin of the GMR effect. The MR ratio and the temperature where the maximum GMR effect is observed seem to be controlled by the distortion or bending of the Mn–O–Mn bond through modifications of the exchange coupling [21,22]. This in turn will have a strong influence on the magnetic interactions. GMR effects in multilayers and heterogeneous alloys (superparamagnetic precipitate in a nonmagnetic metallic matrix) have been ascribed to spin dependent scattering near the interface between the ferromagnetic and nonmagnetic phases [12,23]. In the manganese based perovskite oxides studied here this effect could be due to scattering at the interfaces between antiferromagnetic and ferromagnetic domains and the MR ratio may depend on the concentration of such interfaces. From the magnetization data, it has been seen that antiferromagnetic interactions are nonexistent in sample B. This may explain the small value for the MR observed for this sample. Another significant result for this sample is its transition near 260 K compared to much lower transition temperatures for other samples with the same nominal composition and with yttrium, erbium and ytterbium substitutions. This transition (which corresponds to the ferromagnetic to paramagnetic transition) strongly depends upon the strength of the magnetic interaction Mn^{3+}–O^{2-}–Mn^{4+} and hence on Mn–O–Mn distance and bond angle. The Mn–O–Mn distance and angle in these perovskite structures is a strong function of the tolerance factor. As the tolerance factor decreases the structure becomes more distorted and the MnO_6 octahedra tilt and rotate in order to fill the available space around the rare earth ion, resulting in a smaller Mn–O–Mn bond angle [21]. Among the three samples given in Table 1, sample B has the highest tolerance factor. Therefore, the Mn–O–Mn bond angle has the smallest deviation from 180°, this supports the assumption of enhanced magnetic interactions. Another noteworthy difference between Bi and the other A site substitutions lies in the value of the electronegativity (EN). The EN for Bi is 2.02 compared to La (1.08), Yb (1.1), Er (1.24) and Y (1.22). The strong electron attracting power of Bi provides support to our conjecture of an enhanced interaction. Also, the lower resistivity of sample B can be explained on the basis of the higher electronegativity of Bi and the manner in which this influences the band structure [16]. High transition temperatures, between 260 and 300 K, have been reported for $(La_xBi_{1-x})_{0.5}Ca_{0.5}MnO_3$ compounds and the variation in these values has been attributed to differences in the tolerance factor [24]. The transition observed for the present sample B (260 K) lies within the above range. The present observations as well as previous reports [24] indicate that samples with sharp, well defined GMR peaks in the neighborhood of ambient temperature are possible and this is of particular relevance from an applications point of view.

Acknowledgments

This work was supported in part by a grant from the Natural Sciences and Engineering Research Council of Canada.

References

[1] H.Y. Hwang, S.W. Cheong, P.G. Radaelli, M. Marezio and B. Batlogg, *Phys Rev. Lett., 75* (1995) 914.
[2] B. Raveau, A. Maignan and V. Caignaert, *J. Solid State Chem., 117* (1995) 424.
[3] R. Mahesh, R. Mahendiran, A.K. Raychaudhuri and C.N.R. Rao, *J. Solid State Chem., 114* (1995) 297.
[4] H.L. Ju, J. Gopalakrishnan, J.L. Peng, Q. Li, G.C. Xiong, T. Venkatesan and R.L. Greene, *Phys. Rev. B, 51* (1995) 6143.
[5] G.H. Jonker and J.H. VanSanten, *Physica (Utrecht), 16* (1950) 337.
[6] J.B. Goodenough and J.M. Longo, *Landolt–Börnstein Tabellen*, Vol. 3, Springer Verlag, Berlin, 1970, p. 4a.
[7] C. Zener, *Phys. Rev., 81* (1951) 440.
[8] C. Zener, *Phys. Rev., 82* (1951) 403.
[9] H. Yoshizawa, H. Kawano, Y. Tomioka and Y. Tokura, *Phys. Rev. B, 52* (1995) 13 147.
[10] P.G. Radaelli, D.E. Cox, M. Marezio, S.W. Cheong, P.E. Schiffer and A.P. Ramirei, *Phys. Rev. Lett., 75* (1995) 4488.
[11] M.R. Lees, J. Barratt, G. Balakrishnan, D.McK. Paul and M. Yethiraj, *Phys. Rev. B, 52* (1995) 14 303.
[12] R. von Helmolt, J. Wecker, K. Somwer, L. Haupt and K. Bärner, *J. Appl. Phys., 76* (1994) 6925.
[13] S. Jin, H.M. O'Bryan, T.H. Tiefel, M. McCormack and W.W. Rhodes, *Appl. Phys. Lett., 66* (1995) 382.
[14] D. Bahadur, M. Yewondwossen, Z. Koziol, M. Foldeaki and R.A. Dunlap, *J. Phys. Condens. Matter, 8* (1996) 5235.
[15] R.D. Shannon and C.T. Prewitt, *Acta. Cryst. B, 25* (1969) 925.
[16] Z. Zustao and R. Yufang, *J. Solid State Chem., 121* (1996) 138.
[17] A.K. Srivastava, C.M. Srivastava, R. Mahesh and C.N.R. Rao, *Solid State Commun., 99* (1996) 161.
[18] D. Bahadur, C.M. Srivastava, M.H. Yewondwossen and R.A. Dunlap, *J. Phys. Condens. Matter, 7* (1995) 9883.
[19] D.J. Webb and S.M. Bhagat, *J. Magn. Magn. Mater., 42* (1984) 109.
[20] S.E. Loftland, S.M. Bhagat, H.L. Ju, G.C. Xiong, T. Venatesan and R.L. Greene, *Phys. Rev. B, 52* (1995) 15 058.
[21] J.B. Torrance, P. Lacorre, A.I. Nazzal, E.J. Ansaldo and Ch. Niedermayer, *Phys. Rev. B, 45* (1992) 8209.
[22] J. Fontcuberta, B. Martinez, A. Seffar, S. Pinol, J.L. Garcia-Munoz and X. Obradors, *Phys. Rev. Lett., 76* (1996) 1122.
[23] M.N. Baibich, J.M. Broto, A. Fert, F. Nguyen Van Dau, F. Petroff, P. Etienne, G. Creutzet, A. Friederich and J. Chazelass, *Phys. Rev. Lett., 61* (1988) 2472.
[24] V.A. Bokov, N.A. Grigoryan, M.F. Bryzhina and V.V. Tikhonov, *Phys. Stat. Sol., 28* (1968) 835.